RESEARCH ARTICLE

American Journal of Botany

Bioclimatic factors at an intrabiome scale are more limiting than cyanobiont availability for the lichen-forming genus *Peltigera*

Jade Lu[1], Nicolas Magain[1], Jolanta Miadlikowska[1,4], Jessica R. Coyle[2], Camille Truong[1,3], and François Lutzoni[1]

Manuscript received 4 February 2018; revision accepted 25 April 2018.

[1] Department of Biology, Duke University, Durham, North Carolina 27708, USA

[2] Department of Biology, Stanford University, Stanford, California 94305, USA

[3] Instituto de Biología, Universidad Nacional Autónoma de México (UNAM), C.P. 04510, Mexico City, Mexico

[4] Author for correspondence (e-mail: jolantam@duke.edu)

Citation: Lu, J., N. Magain, J. Miadlikowska, J. R. Coyle, C. Truong, and F. Lutzoni. 2018. Bioclimatic factors at an intrabiome scale are more limiting than cyanobiont availability for the lichen-forming genus *Peltigera*. *American Journal of Botany* 105(7): 1198–1211.

doi:10.1002/ajb2.1119

PREMISE OF THE STUDY: Factors shaping spatiotemporal patterns of associations in mutualistic systems are poorly understood. We used the lichen-forming fungi *Peltigera* and their cyanobacterial partners *Nostoc* to investigate the spatial structure of this symbiosis at an intrabiome scale and to identify potential factors shaping these associations.

METHODS: Ninety-three thalli were sampled in Québec, Canada, along a south–north and an east–west transect of ~1300 km each. We identified the two main partners (*Peltigera* species and *Nostoc* phylogroups) using molecular markers and modeled the effects of environmental variables and partner occurrence on *Peltigera*–*Nostoc* distributions.

KEY RESULTS: *Peltigera* species showed a high degree of specialization toward cyanobionts, whereas two *Nostoc* phylogroups dominated both transects by associating with several *Peltigera* species. *Peltigera* species had narrower ranges than these two main cyanobionts. Distributions of three *Peltigera* species were highly associated with precipitation and temperature variables, which was not detected for *Nostoc* phylogroups at this spatial scale.

CONCLUSIONS: For these cyanolichens, factors driving patterns of symbiotic associations are scale dependent. Contrary to global-scale findings, generalist *Peltigera* species were not more widespread within the boreal biome than specialists. *Nostoc* availability was not the only driver of *Peltigera* species' geographic ranges; environmental factors also contributed to their intrabiome distributions. Climatic conditions (especially precipitation) limited the range of some *Peltigera* species more than the range of their cyanobacterial partners at an intrabiome (boreal) scale.

KEY WORDS boreal biome; cyanobiont; factors shaping spatial symbiotic associations; lichen; mutualism; *Nostoc*; *Peltigera*; symbiotic specificity.

Interspecies associations have extensive implications for evolutionary and ecological success in all ecosystems, as organisms are constantly being shaped by their biotic and abiotic interactions (Thompson, 2005). Of the many types of interactions among organisms, obligate mutualistic relationships represent some of the closest and most intimate associations (Boucher et al., 1982). Dependence by one symbiotic partner can impose selective forces on both partners (i.e., coevolution). These interactions are mediated by abiotic factors (e.g., climate) and can differ greatly geographically (Thompson, 2005).

Lichens have long been considered and studied as model examples of mutualistic symbioses (Nash, 2008). With rare exceptions in Ostropales (Wedin et al., 2004; Baloch et al., 2010) where a loss of lichenization occurred (Lutzoni et al., 2001), the fungal partner (mycobiont) is always found in nature in association with a photosynthesizing partner (photobiont). In some cases, a secondary mycobiont (e.g., Basidiomycota yeast; Spribille et al., 2016) or photobiont (e.g., green alga and cyanobacterium together; Miadlikowska and Lutzoni, 2004) is part of the same lichen thallus. Because lichens are associations between heterotrophs (fungi), photoautotrophs (green algae and cyanobacteria), and sometimes organisms that fix atmospheric dinitrogen (cyanobacteria [Hodkinson et al., 2014; Darnajoux et al., 2017] and members of the Rhizobiales [Hodkinson and Lutzoni, 2009; Hodkinson et al., 2012]), they are ecologically successful in a wide variety of environments, including inhospitable areas such as hot deserts and cold polar regions (Cornelissen et al., 2001; Nash, 2008).

The study of interspecies specificity (here restricted to the main lichen partners), defined as the number of partner species that are selected by one species throughout its geographic range, is essential for a comprehensive understanding of the lichen symbiosis (Otálora et al., 2010) and other symbioses in general. The specificity of lichen-forming fungal species and their main photobionts ranges from strict specialists (associating with only one species) to moderate specialists (associating consistently with a few species) to broad generalists (associating with many species with little or no apparent selectivity). In general, the fungal partner of lichens has a higher degree of specificity in choosing a photobiont than the photosynthetic partner, which has a lower degree of specificity toward mycobionts (e.g., Paulsrud and Lindsblad, 1998; Yahr et al., 2004; O'Brien et al., 2013; Magain et al., 2017a).

There are advantages and disadvantages at both ends of the spectrum. Higher specificity is thought to allow a partner to optimize the benefits obtained from the other partner, while low specificity can allow a partner to occupy more ecological niches (de Vienne et al., 2013). Although it is not entirely clear why mycobionts are usually specialists whereas photobionts are often generalists, several factors seem to be implicated in this pattern. It has been hypothesized that abundance can determine interaction frequency between species, because a relatively abundant species will have frequent encounters with many other individuals of different species (Vasquez et al., 2007). Photobionts are much more widespread and common than their mycobiont counterparts (Werth, 2011), which may lead to increased interaction frequency and generalist behavior. Interaction frequency can be considered a proxy for ecological effect, given that the most prevalent entity in a biological system is thought to create disproportionate influence (Vermeji, 1999, 2004). This is found to be the case in lichens especially at a small spatial scale, as photobionts are thought to have disproportionate influence over mycobionts, such that mycobionts are more dependent on photobionts for survival (Magain et al., 2017a; Chagnon et al., 2018). Mycobionts thus often experience stronger pressure to adapt to a photobiont, which may contribute to their specificity (Chagnon et al., 2018).

Because these factors are not the only ones in play, the general trend of high mycobiont specificity and low photobiont specificity is not always observed. Mycobiont species have been found to associate with multiple photobiont phylogroups, which were used as proxies for species in the case of cyanobacteria (e.g., O'Brien et al., 2005; Magain et al., 2017a, b). The drivers of variation in interaction specificity have yet to be fully elucidated, but this variation has been linked to an interplay of genetically and environmentally based factors. For example, a harsher regional climate may result in selective pressures toward greater flexibility in mycobiont partner choice (Wirtz et al., 2003; Pérez-Ortega et al., 2012; Singh et al., 2016). When a mycobiont lineage is colonizing a new biogeographic zone with a different set of potential partners, flexibility in partner selection may be more beneficial, initially, than being a strict specialist (Singh et al., 2016; Magain et al., 2017a). However, long periods of evolutionary time may shift the pattern toward specialization, as the mycobiont experience differential fitness with different partners under the same environmental conditions. This may result in a mycobiont species associating selectively with one or a few closely related and ecologically adapted (e.g., to water or sun exposure) photobiont phylogroups (Peksa and Škaloud, 2011; Magain et al., 2017a).

The genus *Peltigera* Willd. presents an interesting system for analyzing association specificity and has been the subject of several evolutionary studies at different temporal and spatial scales, designed to reveal patterns of association between symbionts. Some *Peltigera* species are strict specialists (i.e., only found to associate with one *Nostoc* Vaucher ex Bornet and Flahault phylogroup throughout their distribution), while others are broad generalists and associate with many *Nostoc* phylogroups (Magain et al., 2017a).

According to the worldwide study by Magain et al. (2017a, b), the geographic ranges of highly specialized *Peltigera* species in section *Polydactylon* seem to be limited by their partnering *Nostoc*'s distribution, whereas generalist *Peltigera* species, or species associating with different phylogroups in different regions (local specialists; as reported by Blaha et al. [2006] and Nelsen and Gargas [2009]), can spread across wider and more diverse geographic regions through their multiple associations. At a global geographic scale, distributions of *Nostoc* phylogroups seem to be highly dependent on climatic factors (Magain et al., 2017a).

A key element in understanding the evolution of generalist lichen-forming fungi may be host switches from one photobiont to another when they reach the limit of the distribution of one photobiont, resulting in an extension of the mycobiont's distribution range (de Vienne et al., 2013). This may be the predominant evolutionary mechanism shaping symbiotic associations, given that cospeciation, in which the two partners diverge together, appears to be relatively rare (de Vienne et al., 2013; Singh et al., 2016). This is supported by Magain et al. (2017a), in that some *Peltigera* species seem to switch among a few closely related *Nostoc* phylogroups from biome to biome but do not cospeciate. On a smaller and less variable geospatial scale, different evolutionary mechanisms might be at play (i.e., mycobiont selectivity and ranges of cyanobiont partners may not be the limiting factors of distribution as is the case at a global spatial scale).

We analyzed patterns of association of *Peltigera* species and their *Nostoc* partners (identified on the basis of ITS and *rbcLX* loci, respectively) along two transects of nearly 1300 km each (south–north and east–west) in the boreal biome. We examined potential drivers (environmental variables vs. presence of symbiont vs. both factors) of each partner's distribution using linear mixed models. Specifically, we sought to answer the following questions: (1) Does the distribution of *Nostoc* phylogroups determine the distribution of *Peltigera* species in the boreal biome? (2) Does an abiotic climatic gradient drive patterns of associations or symbiont distributions in this biome? (3) Do global patterns of association and specificity hold true within this biome?

MATERIALS AND METHODS

Sampling

In August 2011, sampling was conducted along two transects (south–north [SN] and east–west [EW]) that crossed the circumboreal belt in Québec, Canada. On the SN transect, there were nine major equidistant localities (~160 km apart) ranging from 46.77°N, 73.01°W (SN1) to 57.91°N, 72.98°W (SN9), spanning ~1300 km from the southern limit of the boreal biome (Canadian Shield) to the tree limit (Fig. 1). Specimens of *Peltigera* were found and collected in eight localities (Appendix 1), from the

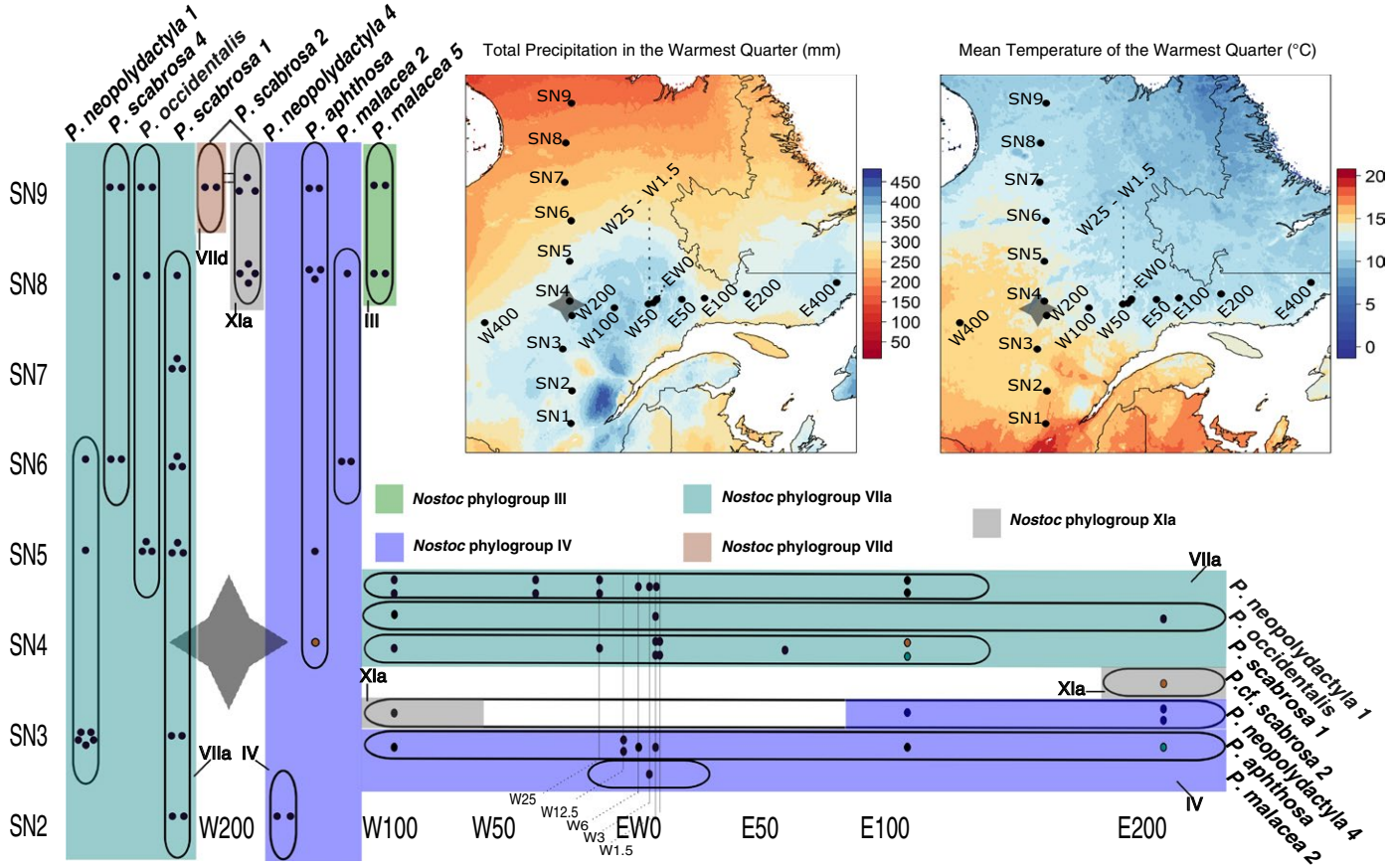

FIGURE 1. (Top right) The two physical maps show precipitation and temperature gradients in the area spanned by the south–north (SN) and east–west (EW) transects. Sampling localities along both transects are represented by abbreviations SN1–SN9 and W400–E400. (Left and bottom) Vertical and horizontal bands show *Peltigera* spp. distributions and associations with *Nostoc* cyanobionts across the latitudinal (SN) and longitudinal (EW) transects in Québec, Canada. Some localities, such as SN1, W400, and E400, are not shown because no *Peltigera* thalli were found at those localities. *Peltigera* species are labeled and their ranges are represented by solid lines. Colored bands represent *Nostoc* phylogroups as shown in the key and in Fig. 3. Black dots indicate specimens for which both partners, mycobiont and cyanobiont, were identified on the basis of ITS and *rbcLX* sequences, respectively. Colored dots represent specimens with missing ITS (red) or *rbcLX* (green) sequences. Longitude of W200 is approximated by the longitude of SN4 as shown by the large gray star, which also depicts where the EW transect crosses the SN transect.

second-most southern locality (SN2: 48.63°N, 73.04°W) to the northernmost locality (SN9: 57.83°N, 73.19°W). Within each of these eight localities, sampling was systematically conducted at three sites (west [W], central [C], and east [E]) arranged linearly and separated by 3.2 km from the central site. Within each of the three sites we explored three clusters (W1, W2, W3; C1, C2, C3; E1, E2, E3) of 20 m in diameter each, placed ~10 m apart. The EW transect was located roughly at the latitude of SN4 (51.03°N). The central locality along the EW transect (EW0: 51.11°N, 68.52°W) was ~320 km to the east of SN4 (Fig. 1). East–west localities ranged from 2.4 km (1.5 miles) to 640 km (400 miles) away from EW0. The EW transect spanned ~1300 km from the westernmost (W400: 50.28°N, 77.50°W) to the easternmost locality (E400: 51.68°N, 59.15°W). *Peltigera* specimens were found and collected from 11 localities ranging from W100 (50.53°N, 70.74°W) to E200 (51.28°N, 63.84°W). Along the EW transect, each locality was represented by only one site (C), and similar to the SN transect, we explored three clusters (C1, C2, C3) of 20 m in diameter each, placed ~10 m apart. Lobes were taken from 93 *Peltigera* thalli from these 19 localities (35 sites and 105 clusters) and air dried before processing for molecular work. All these specimens were deposited at DUKE (Appendix 1).

Data collection

DNA was extracted from 77 lichen specimens (16 specimens were already included in Magain et al. [2017a]) using a standard phenol-chloroform DNA isolation protocol with 2% SDS buffer (Zolan and Pukkila, 1986). The internal transcribed spacer (ITS) of the nuclear ribosomal RNA tandem repeats was selected to characterize mycobiont populations because it is highly variable at the species level in *Peltigera* (Miadlikowska et al., 2003; O'Brien et al., 2009) and has been used as a universal DNA barcode for fungi (Schoch et al., 2012). This region was amplified successfully for 74 specimens using polymerase chain reaction (PCR) with the primers ITS1F (Gardes and Bruns, 1993) and ITS4 (White et al., 1990) following Magain et al. (2017a).

For the cyanobacterial photobiont *Nostoc*, *rbcLX*—which includes the last 82 amino acids of the RUBISCO large subunit (*rbcL*), a putative chaperone gene (*rbcX*), and two intergenic spacers (Li

and Tabita, 1997)—was amplified and sequenced for 75 specimens using the primers CX and CW (Rudi et al., 1998) as described in O'Brien et al. (2013). Both ITS and *rbcLX* were successfully sequenced for 72 of the 77 sampled specimens.

The PCR products were purified with ExoSAP (Afymetrix, Santa Clara, California, USA) following the manufacturer's protocol and sequenced as described in Magain et al. (2017a) at the Duke Genome Sequencing and Analysis Core Facility of the Institute for Genome Sciences and Policies. All newly generated ITS (74 sequences) and *rbcLX* (75 sequences) data were deposited in GenBank (Appendix 1). Sequences of each locus (ITS and *rbcLX*) from 16 specimens were already deposited in GenBank by Magain et al. (2017a).

Alignments

All sequences were subjected to BLASTn searches (Wheeler et al., 2007) to confirm the fungal or cyanobacterial origin of each sequence fragment. They were assembled (visually inspected and manually corrected when necessary) using Sequencher version 5.0.1 (Gene Codes Corporation, Ann Arbor, Michigan, USA) and aligned using MacClade version 4.08 (Maddison and Maddison, 2005). The "Nucleotide with AA color" option was used for guiding the *rbcLX* alignment. Sequencing reactions of *rbcLX* produced clean reads without evidence of secondary peaks, suggesting that a single photobiont genotype dominated in each of the lichen thalli. Ambiguously aligned regions were delimited manually following Lutzoni et al. (2000) and were excluded from phylogenetic analyses.

Phylogenetic analyses

We assembled a dataset consisting of 319 *rbcLX* sequences of free-living and symbiotic *Nostoc* spp. from GenBank in addition to the 16 already published and 75 newly generated sequences from the transects, for a total of 410 *rbcLX* sequences. Both spacers in *rbcLX* were too variable to be unambiguously aligned across the alignment and were removed from subsequent phylogenetic analyses (696 sites). The final matrix contained 621 nucleotide sites. Maximum likelihood searches for the optimal trees and bootstrap analyses of the cyanobiont sequences were conducted using RAxML version 8.2.10 (Stamatakis, 2006; Stamatakis et al., 2008) as implemented on the CIPRES portal (Miller et al., 2010). These searches were conducted with the rapid hill-climbing algorithm for 1000 replicates with the general time reversible (GTR) substitution model (Rodríguez et al., 1990) and gamma distribution parameter approximated with four categories in all analyses. A partition of three subsets corresponding to the first, second, and third codon position of the *rbcLX* was defined.

Haplotype network

Following previous studies (Magain et al., 2017a, b; J. Miadlikowska, unpublished data, for section *Peltidea*), mycobiont species were identified on the basis of their ITS sequences. Separate ITS alignments were prepared for haplotype network analyses on the two *Peltigera* sections, *Polydactylon* Miadlikowska and Lutzoni (798 nucleotide sites) and *Peltidea* (Ach.) Vain. (691 nucleotide sites). The delimitation of the sections of the genus follows Miadlikowska and Lutzoni (2000). Because haplotype network analyses were restricted to each species or small group of closely related species separately, no ambiguity was found in these subalignments and, consequently, all nucleotide sites were used to infer haplotype networks. Haplotype networks were generated using TCS version 1.21 (Clement et al., 2000) based on 69 mycobiont ITS sequences from section *Polydactylon* and 21 mycobiont ITS sequences from section *Peltidea*. We used a parsimony criterion with the 0.95 threshold value, and gaps were considered as a fifth character state.

Modeling *Peltigera–Nostoc* distribution

For each *Peltigera* species that occurred in at least six clusters (*P. aphthosa*, *P. neopolydactyla* 1, *P. occidentalis*, *P. scabrosa* 1, and *P. scabrosa* 2), we modeled the probability of species presence across the study region as a function of climate and the presence of observed *Nostoc* symbiont phylogroups using generalized linear mixed models. We fit three types of models for each species: (1) an environment-only model with linear and quadratic effects of temperature and precipitation from the warmest three months of the year, in which quadratic effects were constrained to be negative so that species responses are concave-down; (2) symbiont-only models, which estimate the effect of each potential *Nostoc* symbiont's presence on the probability of presence; and (3) full models that combine each symbiont-only model with the environment-only model and also include interactive effects of symbiont presence on the response of *Peltigera* species to environmental variables. All models used a Bernoulli likelihood with logit link function and included a random intercept for the effect of locality (to model spatial autocorrelation). We used weakly informative normal and half-normal priors for coefficients and a weakly informative half-Cauchy prior on the standard deviation of the normally distributed random effect of locality. For comparison, we fit the same set of models for each *Nostoc* phylogroup that occurred in at least six clusters (*Nostoc* phylogroups IV, VIIa, and XIa). In this case, the symbiont-only models assess the effect of *Peltigera* species presence on the probability of a *Nostoc* phylogroup's presence.

Climate data were obtained from WorldClim (http://worldclim.org/version2), which interpolates and averages weather station data from 1970 to 2000. We chose total precipitation and mean temperature during the warmest quarter as measures of water availability and thermal environment because these two variables were less correlated than other, similar measures ($r = 0.38$) and because they represent environmental conditions when these lichen thalli are metabolically active. We coded models in Stan (Carpenter et al., 2017) and estimated parameters with the MCMC "No-U-Turn" sampler using the R package "RSTAN" (Stan Development Team 2017) and three sampling chains. Model convergence was checked with standard diagnostic tests, and sampling chains were run until all parameters obtained ≥1000 effective samples. Models were compared with Akaike weight (WAIC) and area under the ROC curve (AUC). Effects of environmental variables were determined visually from plots of conditional posterior predictive distributions.

RESULTS

Data collection

We generated 149 new sequences: 74 ITS sequences from *Peltigera* and 75 *rbcLX* sequences from *Nostoc*. Both ITS and *rbcLX* were obtained for a total of 72 lichen specimens, while two specimens yielded

only ITS sequences, and three specimens yielded only *rbcLX* sequences (Appendix 1). Overall, for the 93 lichen specimens collected along both transects, including already published sequences, 90 ITS sequences of the mycobionts and 91 *rbcLX* sequences of the cyanobionts were included in this study. A total of 88 thalli were represented by sequences of both partners (Appendix 1).

Along the SN transect, mean temperature in the warmest quarter ranged from 15.8°C at the second-most southern locality (SN2) to 11.4°C at the most northern locality (SN9). Total precipitation during the warmest quarter ranged from 181 mm at SN9 to 326 mm at SN3 (Fig. 1). Although less variable, climatic factors were not entirely even longitudinally. Temperature ranged from 11.5° to 13.1°C, and precipitation ranged from 309 mm to 354 mm within the EW transect (Fig. 1).

Peltigera haplotype network

In total, nine *Peltigera* species (*sensu* Magain et al., 2017b) belonging to sections *Peltidea* and *Polydactylon* (Miadlikowska and Lutzoni, 2000) were detected in the sampled material for this project (Fig. 2). These nine species represent five traditional morphospecies names: *Peltigera aphthosa* (L.) Willd., *P. malacea* (Ach.) Funck, *P. neopolydactyla* (Gyeln.) Gyeln., *P. occidentalis* (A.E. Dahl) Kristinsson, and *P. scabrosa* Th. Fr. Section *Polydactylon* included 71 specimens from six species (Fig. 2), which were identified in accordance with Magain et al. (2017b) on the basis of ITS sequence comparisons. There were six specimens of *Peltigera neopolydactyla* 4, representing two haplotypes separated by one mutation. One of the two haplotypes was prevalent because it was found in five of the six specimens sampled for this species (Fig. 2). The nine sequenced specimens of *P. scabrosa* 2 belong to three haplotypes, two common (n = 4) and one rare (n = 1; Fig. 2). *Peltigera scabrosa* 1 encompassed 22 sequenced specimens (Fig. 2), which split into two haplotypes: one common haplotype found in 18 specimens and a less common haplotype found in four specimens. A total of five specimens were identified as *P. scabrosa* 4, all belonging to the same haplotype. Similarly, *P. occidentalis* and *P. neopolydactyla* 1 were represented by one haplotype comprising nine and 18 specimens, respectively (Fig. 2).

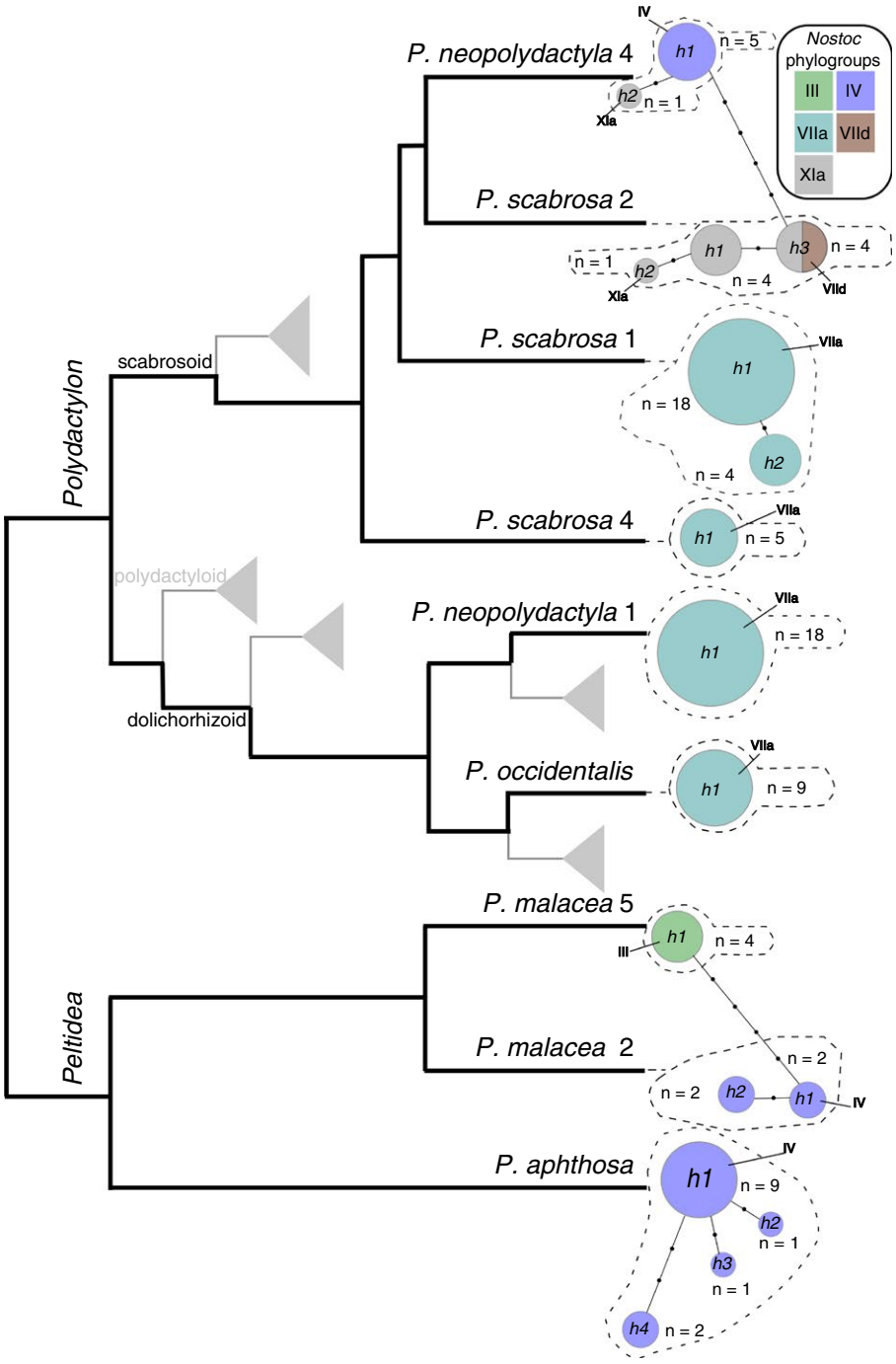

FIGURE 2. Schematic cladogram (in black) depicting relationships among nine putative *Peltigera* species from two sections, *Peltidea* and *Polydactylon*, sampled for this study (adapted from Magain et al., 2017a; J. Miadlikowska, unpublished data). Gray lines and triangles indicate placements of the remaining species included in section *Polydactylon* (Magain et al., 2017a, b), not sampled in this study. ITS haplotype networks of sampled *Peltigera* species are shown at the tip of the terminal branches. Each circle represents a unique ITS haplotype, and its size is proportional to the number of included specimens (n); black dots indicate the number of mutations between haplotypes. Colors represent, proportionally, the *Nostoc* phylogroups (as delimited in Fig. 3) associated with each *Peltigera* haplotype.

Section *Peltidea* accounted for a total of 22 specimens representing three species (Fig. 2), which were identified in accordance with Miadlikowska and Lutzoni (2000) and more recent analyses (J. Miadlikowska, unpublished data) based on ITS sequence similarity. *Peltigera aphthosa* encompassed 14 specimens (one was identified based solely on morphology), representing four haplotypes with one being prevalent (n = 9).

Specimens of *P. malacea* sensu lato corresponding to *P. malacea* 2 (J. Miadlikowska, unpublished data) are represented by four sequences from two haplotypes, while all four specimens of *P. malacea* 5 (J. Miadlikowska, unpublished data) had identical ITS sequences (Fig. 2).

Nostoc identity

Based on the global *rbcLX* phylogeny of *Nostoc* (Appendix S1, see Supplemental Data with this article), a total of five phylogroups from *Nostoc* clade 2 (*sensu* Otálora et al., 2010) were identified in accordance with O'Brien et al. (2013) and Magain et al. (2017a) (Fig. 3). These phylogroups were well supported (bootstrap values >70%), except for phylogroup IV. *Nostoc* phylogroups III and IV, both from *Nostoc* clade 2, subclade 2, were found in four and 22 specimens, respectively (Figs. 2 and 3). Within subclade 3, which contains most lichenized cyanobacteria (Otálora et al., 2010; Magain et al., 2017a), *Nostoc* phylogroup VIIa was the most commonly sampled (from 54 specimens), whereas closely related phylogroup VIId was found only in two specimens and the more distant *Nostoc* phylogroup XIa was found in eight thalli (Figs. 2 and 3).

Peltigera–Nostoc associations

The nine *Peltigera* species and five *Nostoc* phylogroups formed 11 symbiotic pairs. *Nostoc* phylogroups were found to be symbionts of one to four *Peltigera* species, whereas *Peltigera* species were found in association with one or two phylogroups (Figs. 1 and 2). At the section level, the six species from section *Polydactylon* are associated with nearly all *Nostoc* phylogroups, except phylogroup III (Figs. 2 and 3). All sequenced specimens of *P. scabrosa* 1 (n = 22), *P. scabrosa* 4 (n = 5), *P. neopolydactyla* 1 (n = 18), and *P. occidentalis* (n = 9) were found in association only with phylogroup VIIa. *Peltigera scabrosa* 1 spanned almost the entirety of both transects as one of the most widespread species in this sampling (i.e., across SN2–SN8 in latitude and W100–E100 in longitude) (Fig. 1). Individuals of *P. scabrosa* 4 were found only in the northern portion of the SN transect (SN6–SN9), and this species was not collected on the longitudinal transect that is located approximately at the latitude of SN4 (Fig. 1). *Peltigera neopolydactyla* 1 ranged from SN3 to SN6 and from W100 to E100 (Fig. 1), whereas *P. occidentalis* ranged from SN5 to SN9 and from W100 to E200. Both were thus fairly widespread, especially on the EW transect.

Specimens of *P. scabrosa* 2, which were confined to the northern portion of the SN transect (SN8 and SN9), occurred in association with two cyanobionts, *Nostoc* phylogroups XIa and VIId (Figs. 1 and 2). An individual collected at E200, morphologically identified as *P. scabrosa* 2, was found in association with a cyanobiont from phylogroup XIa. Given that the latitude of the EW transect can be roughly approximated by the latitude of SN4, E200 was the most southern point at which *P. scabrosa 2* was found. Unfortunately, the identification of this specimen at E200 could not be confirmed with DNA sequencing because the ITS sequencing failed.

Peltigera neopolydactyla 4 was restricted to the southern parts of the SN transect, with samples collected at the most southern locality, SN2. However, *P. neopolydactyla* 4 was found multiple times on the EW transect and ranged from E200 to W100, and was also present in the SN transect, corresponding approximately to W200 in longitude. These specimens associated with phylogroup IV, with one exception of an individual collected at W100 that was found in association with phylogroup XIa (Figs. 1–3).

Species from section *Peltidea* associated with two *Nostoc* phylogroups (III and IV; Figs. 2 and 3) from clade 2, subclade 2 (section *Peltidea* was not found in association with cyanobionts from subclade 3). All sequenced *P. aphthosa* samples were associated with *Nostoc* phylogroup IV. Distribution of these specimens ranged from SN4 to SN9 on the latitudinal transect and from W100 to E200 on the longitudinal transect. *Peltigera malacea* 2, also associated with *Nostoc* phylogroup IV, spanned SN6–SN8 in latitude and was found at W3 (corresponding to the latitude of SN4; Fig. 1). *Peltigera malacea* 5 was found in association with *Nostoc* phylogroup III at the northernmost localities, SN8 and SN9 (Fig. 1).

The *Nostoc* phylogroups also had variable distributions, although not as scattered as the *Peltigera* species (Fig. 1). *Nostoc* phylogroups VIIa and IV have widespread distributions across both transects and associate with multiple *Peltigera* species (four and three, respectively; Fig. 1). *Nostoc* phylogroups VIId and III have limited northern distributions (SN8 and SN9) and associate only with *P. scabrosa* 2 and *P. malacea* 5, respectively (Fig. 1). The presence of these two phylogroups in the northernmost localities results in a higher *Nostoc* diversity in the northern portion of the SN transect. Phylogroup XIa, by contrast, has a relatively scattered distribution. It was found in the northernmost localities of the SN transect with *P. scabrosa* 2 and at both edges of the EW transect in association with *P. scabrosa* 2 and *P. neopolydactyla* 4.

Predicted occurrence of *Peltigera* and *Nostoc* partners

In all cases, full models including both environmental covariates and the effect of symbiont presence performed better than environment-only or symbiont-only models (Table 1), except in the case of *P. scabrosa* 2, for which inclusion of the presence of *Nostoc* VIId did not improve the predictive ability of the model. Therefore, hereafter we interpret species responses to climate gradients from predictions of the full models. In the full models, three *Peltigera* species responded to environmental gradients. Models predict that, when the *Nostoc* symbiont is present at a locality, *P. neopolydactyla* 1 is more likely to occur at wetter sites, *P. occidentalis* is less likely to occur at the wettest sites, and *P. scabrosa* 1 is more likely to occur in the middle of the precipitation gradient (Fig. 4A). Each of these three species was found exclusively in association with the same *Nostoc* phylogroup VIIa. *Peltigera scabrosa* 2 is unlikely to occur at warm-temperature sites, whereas the other taxa show only weak responses to temperature but are generally more likely to occur in the middle of the temperature gradient (Fig. 4B). In general, precipitation and temperature did not have consistent effects on

FIGURE 3. Global phylogenetic tree of *Nostoc* based on a maximum likelihood analysis of 410 *rbcLX* sequences representing free-living and symbiotic *Nostoc*, including 91 cyanobionts from lichen thalli collected along both transects (south–north and east–west) in Québec, Canada. Thick branches received bootstrap values >70%. Clades and subclades were delimited following Otálora et al. (2010). A detailed view of this phylogenetic tree, including support values, taxon names, and GenBank accession numbers for all terminals, is provided in Appendix S1. Phylogroups sampled in this study are highlighted by colored boxes. Phylogroups were numbered following Magain et al. (2017a). Two terminal branches were truncated, as indicated by a folding symbol.

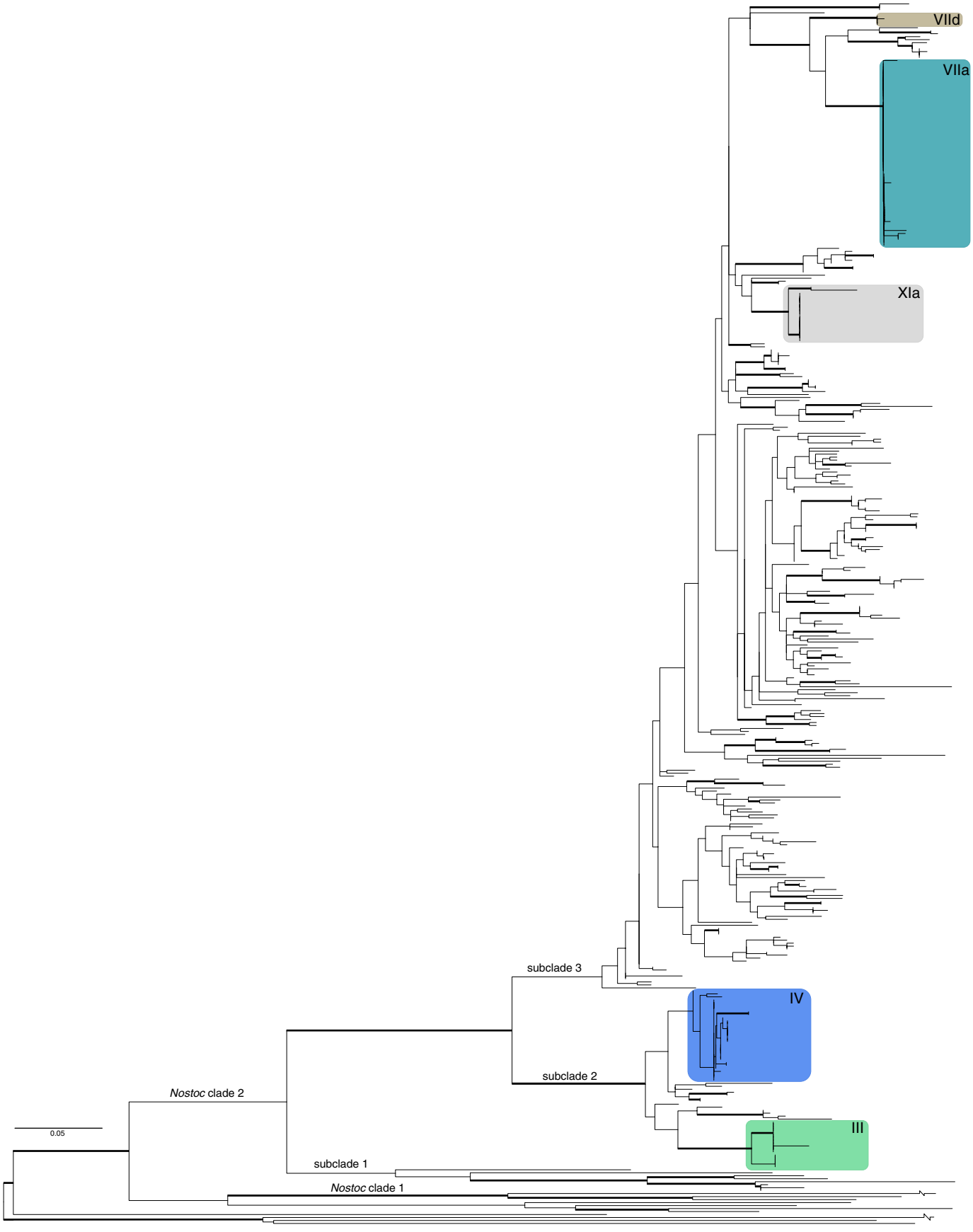
VIId
VIIa
XIa
subclade 3
IV
subclade 2
III
Nostoc clade 2
0.05
subclade 1
Nostoc clade 1

TABLE 1. Comparison of models predicting the presence of *Peltigera* species and *Nostoc* phylogroups. "Focal species" is the species whose occurrence was modeled. "Symbiont" indicates which potential symbiont was included as a covariate in the full and symbiont-only models. AUC is the area under the ROC curve. Within each focal species, models are ranked by increasing Akaike weight (WAIC; best to worst).

Focal species	Symbiont	Model	AUC	WAIC	Model rank
P. aphthosa	*Nostoc* IV	Full	0.99	17.2	1
		Environment-only	0.80	55.1	2
	Nostoc IV	Symbiont-only	0.91	66.2	3
P. neopolydactyla 1	*Nostoc* VIIa	Full	0.95	34.2	1
		Environment-only	0.92	41.8	2
	Nostoc VIIa	Symbiont-only	0.28	70.8	3
P. occidentalis	*Nostoc* VIIa	Full	0.96	23.6	1
		Environment-only	0.89	39.0	2
	Nostoc VIIa	Symbiont-only	0.69	51.4	3
P. scabrosa 1	*Nostoc* VIIa	Full	0.90	50.1	1
		Environment-only	0.87	58.0	2
	Nostoc VIIa	Symbiont-only	0.74	79.3	3
P. scabrosa 2	*Nostoc* XIa	Full	1.00	5.8	1
	Nostoc VIId	Full	0.95	23.0	2
		Environment-only	0.95	23.5	3
	Nostoc XIa	Symbiont-only	0.88	51.3	4
	Nostoc VIId	Symbiont-only	0.39	51.4	5
Nostoc IV	*P. aphthosa*	Full	0.98	24.7	1
	P. malacea 2	Full	0.90	52.0	2
	P. neopolydactyla 4	Full	0.85	57.0	3
		Environment-only	0.85	65.4	4
	P. aphthosa	Symbiont-only	0.80	81.7	5
	P. malacea 2	Symbiont-only	0.59	81.7	5
	P. neopolydactyla 4	Symbiont-only	0.37	81.8	7
Nostoc VIIa	*P. occidentalis*	Full	0.98	24.1	1
	P. neopolydactyla 1	Full	0.96	32.1	2
	P. scabrosa 4	Full	0.96	33.8	3
	P. scabrosa 1	Full	0.96	33.9	4
		Environment-only	0.94	41.2	5
	P. neopolydactyla 1	Symbiont-only	0.69	78.0	6
	P. occidentalis	Symbiont-only	0.39	78.0	6
	P. scabrosa 1	Symbiont-only	0.75	78.0	6
	P. scabrosa 4	Symbiont-only	0.45	78.0	6
Nostoc XIa	*P. scabrosa* 2	Full	0.99	10.6	1
	P. neopolydactyla 4	Full	0.93	26.3	2
		Environment-only	0.90	31.2	3
	P. neopolydactyla 4	Symbiont-only	0.41	47.7	4
	P. scabrosa 2	Symbiont-only	0.92	47.7	4

the distribution of *Nostoc* taxa among models including different *Peltigera* symbionts, although models of *Nostoc* phylogroup IV predicted a lower probability of occurrence at high-temperature sites (Appendices S2 and S3).

DISCUSSION

Our findings were largely aligned with the traditional paradigm that mycobiont species show a higher degree of specialization than their photobiont partners (e.g., Beck et al., 2002; Yahr et al., 2004; O'Brien et al., 2005, 2013; Myllys et al., 2006; Magain et al., 2017a). Furthermore, we found consistent associations between previously studied *Peltigera* species and *Nostoc* phylogroups with no novel mycobiont–cyanobiont pairings (O'Brien et al., 2013; Magain et al., 2017a, b). The two most common *Nostoc* cyanobionts (phylogroups IV and VIIa) were associated with seven of the nine *Peltigera* species sampled for this study (Fig. 2). None of the *Peltigera* species were present along the entire length of either the longitudinal or latitudinal transect. Some species were widespread (e.g., *P. scabrosa* 1) while others were limited to certain areas, mostly restricted to the southern (*P. neopolydactyla* 4) or northern (*P. scabrosa* 2 and *P. malacea* 5) ends of the latitudinal transect. By contrast, the two most common cyanobionts, *Nostoc* phylogroups VIIa and IV, were found throughout both transects where *Peltigera* thalli were sampled (Fig. 1).

Asymmetric specificity associated with ecological success of *Peltigera* lichens

At this intrabiome spatial scale, the common *Nostoc* phylogroups and their interactions with *Peltigera* species displayed a pattern of asymmetrical specialization—highly specialized mycobionts associating with generalist photobionts (Figs. 1 and 2). This has been found to indicate the heavy influence that the generalist photobiont partner wields over the specialist mycobiont, in an evolutionary and ecological sense (Chagnon et al., 2018). This unequal influence mirrors the asymmetrical dependence of these associations; *Peltigera*

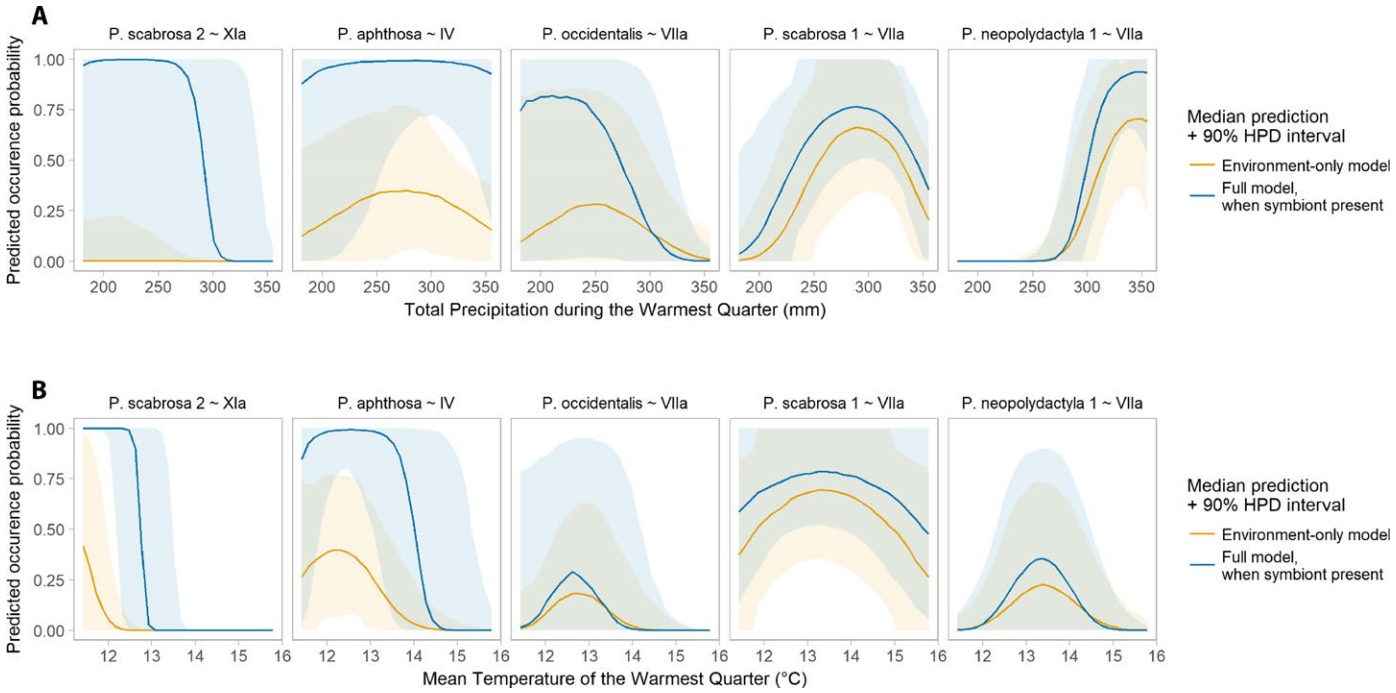

FIGURE 4. Predicted effect of (A) precipitation and (B) temperature on the probability of *Peltigera* species presence. Lines indicate the median of the posterior predictive distribution from the full (blue) and environment-only (yellow) models. In A, model predictions are conditional on precipitation held constant at its mean value across sites (290 mm), whereas in B, model predictions are conditional on temperature held constant at its mean value across sites (12.7°C). The full model prediction is conditional on the *Nostoc* symbiont being present at the locality. The label at the top of each panel indicates which *Nostoc* phylogroup was included as a predictor in the full model. Model predictions are shown with 90% highest posterior density (HPD) intervals.

(never found free living) is much more dependent on *Nostoc* (found free living; O'Brien et al., 2005; Zúñiga et al., 2017) than vice versa. In the case of *Nostoc* phylogroup VIIa, there are four *Peltigera* species that are highly dependent and exclusively interacting with this phylogroup (Figs. 1 and 2). As shown in Magain et al. (2017a, b) based on the complete phylogeny of section *Polydactylon*, these four species belong to two different major lineages in the section: the dolichorhizoid (*P. neopolydactyla* 1 and *P. occidentalis*) and scabrosoid (*P. scabrosa* 1 and 4) clades (Fig. 2). It is thus possible that the fungal partner speciated while the *Nostoc* phylogroup did not, resulting in an increasingly more generalist *Nostoc* symbiont, as suggested by Singh et al. (2016) for lichenized fungi associated with the green alga *Trebouxia*. For these four *Peltigera* species, there seems to be no selective pressure for the *Nostoc* phylogroup to diverge, as the fungal partner continues to be dependent on this *Nostoc* phylogroup. Overall, our results suggest that *Peltigera* species have a narrower ecological range than *Nostoc* phylogroups at this intrabiome scale. The observed high specialization and narrow spatial range of *Peltigera* within the boreal biome, and the larger geographic range of cyanobiont phylogroups IV and VIIa compared to most *Peltigera* species, suggests that the spatial distribution of *Peltigera* species is very likely shaped by other factors (environmental variables) in addition to the presence–absence of their cyanobionts at this intrabiome scale.

Spatial scales matter

The finding of Magain et al. (2017a) at a global spatial scale—that a generalist pattern of association with multiple *Nostoc* phylogroups and local specialization through photobiont switches is associated with larger geographic ranges of the fungal partners—does not appear to hold true at the intrabiome scale. Many of the *Peltigera* species that were found widely distributed along the transects are strict specialists in the area surveyed, such as *P. scabrosa* 1 and *P. aphthosa*. However, this is occurring in an area where their respective cyanobiont phylogroup seems omnipresent, therefore not requiring host switches. Moreover, it should be noted that specialists in this context are not necessarily global specialists. Cyanobiont switches have been reported for species such as *P. neopolydactyla* 1 and *P. occidentalis* across bioclimatic zones (Magain et al., 2017a). For example, these two species, always found in association with *Nostoc* phylogroup VIIa along the SN and EW transects, and overall across the boreal biome, were associated with phylogroup VIIb in the Appalachian Mountains (Magain et al., 2017a). Therefore, within the boreal biome, cyanobiont switches do not seem to play a large role in shaping patterns of associations, except at the border with another biome (e.g., the Arctic; Fig. 1). A potential case of *Nostoc* switch may be *P. scabrosa* 2, which is found at lower latitudes with *Nostoc* phylogroup XIa (E200) and with both *Nostoc* phylogroups XIa and VIId at the most northern locality (SN9). It is possible that beyond SN9, in the Arctic biome, *P. scabrosa* 2 might associate more frequently with phylogroup VIId, for example (Figs. 1 and 3). *Peltigera scabrosa* 2 was also reported with phylogroup VIId in other northern areas such as Nunavik and Greenland (Magain et al., 2017a). Even if *P. scabrosa* 2 can associate with two *Nostoc* phylogroups, it does not seem to correlate with a more widespread distribution within the boreal biome (Fig. 1). Similarly, *P. neopolydactyla* 4 was found in association with two *Nostoc* phylogroups but

also showed a limited distribution. These findings are in agreement with a recent study on *Peltigera* and *Nostoc* that found evidence against the hypothesis that generalism allows for niche expansion (Chagnon et al., 2018), showing instead that associating with multiple partners resulted in a "jack-of-all-trades but master of none" scenario, in which a mycobiont's ability to associate with one partner may impair its fitness when associating with another (Wilson and Yoshimura, 1994; Chagnon et al., 2018). This is supported in the present study, in that *Peltigera* species that are not strict specialists still show increased preference for one *Nostoc* phylogroup over others (Fig. 2). A similar pattern was found in a recent study of *Peltigera* and cyanobiont associations in Chile and maritime Antarctica, where mycobionts displayed preference for a specific *Nostoc* through unequal frequencies of association within a climatic zone (Zúñiga et al., 2017).

In finding evidence against the niche-breadth hypothesis, Chagnon et al. (2018) postulated that the range of potential partners does not act as the limiting factor for niche and range expansion for *Peltigera* and *Nostoc*. This appears to be true in our study at the intrabiome scale, for both strict specialists and mycobionts associating with more than one phylogroup. Although, as discussed earlier, some specific *Peltigera–Nostoc* associations are wide ranging in the boreal zone, many are confined to parts of the transect. It is the case throughout much of this sampled region that *Nostoc* distribution is wider than *Peltigera* distribution (Fig. 1). Thus, many *Peltigera* species are restricted in their distribution, even if their photobiont partner is available in surrounding areas. This biome-level finding differs markedly from the global observation that *Nostoc* distributions drive *Peltigera* distribution patterns (Magain et al., 2017a). However, these conclusions are scale dependent. On the global (i.e., interbiome) spatial scale, cyanobiont availability appears to be the limiting factor for niche expansion. Cyanobiont switches allow *Peltigera* to bypass the limitation of a specific *Nostoc* distribution in order to extend their global range (Magain et al., 2017a). It has also been found within fungal–algal lichen associations that low photobiont availability in harsh environmental regions drives associations toward a generalist pattern, again indicating that photobiont availability is the limiting factor (Wirtz et al., 2003; Singh et al., 2016). Both of these outcomes show the dynamic interaction between environmental, evolutionary, and genetically based factors, as well as the importance of spatial scale.

At an intrabiome scale, geographic ranges of *Peltigera* species are shaped more by abiotic factors than by cyanobiont availability

It appears that within the boreal biome, environmental factors have more influence on the spatial range of the fungal partner *Peltigera* than on the *Nostoc* phylogroups. Specifically, latitudinal gradients, especially precipitation (Fig. 4A), seem to have greater impacts on the mycobiont than on the cyanobiont. For example, *P. neopolydactyla* 4 is found only in the southern area of the biome (SN2) and across the EW transect (approximately the latitude of SN4) (Fig. 1). However, *Nostoc* phylogroup IV was found throughout our two transects. It is thus likely that environmental limitations drive the distribution of *P. neopolydactyla* 4. This may indicate that the climatic preferences of *Peltigera* are more restricted within a biome, and that lichen photobionts are more resilient to abiotic factors, than previously indicated. We did not model the presence of *P. neopolydactyla* 4 (and *P. malacea* spp.) because of their limited records. However, the distributions of three more abundant species—*P. neopolydactyla* 1, *P. occidentalis*, and *P. scabrosa* 1—were highly associated with the climate gradient, especially precipitation (Fig. 4A). These three species were found exclusively associated with *Nostoc* phylogroup VIIa, which is present throughout both transects, yet *P. occidentalis* is more likely to occur in dry sites, *P. neopolydactyla* 1 is more likely to occur in wet sites, and *P. scabrosa* 1 is more likely to be found in areas with intermediate levels of precipitation (Fig. 4A). These relatively narrow environmental spectra for lichen-forming fungi associating with the same photobiont could explain their higher species richness compared to their photobionts and could be an important driver of speciation for the genus *Peltigera*. By contrast, only *Nostoc* phylogroup IV showed a slight association with temperature (Appendix S3). Furthermore, models that attempt to predict the distribution of *Peltigera* species solely from the presence of an appropriate *Nostoc* symbiont generally perform poorly within a biome. Comparing the predictions of the full models to those of the models containing only environmental covariates shows that environmental constraints of *Peltigera* species distributions are weaker if the *Nostoc* symbiont is present. In general, models predict a wider range of suitable environmental conditions when the symbiont is present than when symbiont presence is not included as a predictor (Fig. 4). For example, the environment-only model of *P. scabrosa* 2 suggests that this species is unlikely to occur at sites experiencing mean summer temperatures above 12°C. However, when *Nostoc* XIa is present, that threshold shifts up to 13°C (Fig. 4B).

In the present study, a notable case that may indicate more finely tuned environmental preferences is that of putative *P. malacea* 2 and *P. malacea* 5. *Peltigera malacea* 2 was found in association with *Nostoc* phylogroup IV at W3 and from SN6 to SN8, whereas closely related *P. malacea* 5 occurred in the most northern localities, SN8 and SN9, in association with a different *Nostoc* (phylogroup III) despite the presence of phylogroup IV. In this case, it is possible that a speciation event of the mycobiont was associated with a *Nostoc* phylogroup switch. However, to better understand and explain the observed patterns within the *malacea* complex, we need to extend the sampling farther north.

Factors shaping levels of specificity

The conditions for the rare reciprocal one-to-one specificity in species of the genus *Peltigera* are not well known but have been described for certain species of *Collema*, *Leptogium*, and *Degelia* lichens (Otálora et al., 2010, 2013). In those cases, asexual reproduction through codispersal of the mycobiont and the photobiont (i.e., vertical transmission of the photobiont) as well as narrow ecological niches were identified as essential driving factors toward high reciprocal specificity. Given that *P. malacea* sensu lato does not have specialized codispersal structures, O'Brien et al. (2013) proposed that either thallus fragmentation resulting in clonal reproduction or genetically determined specificity drives reciprocal specificity. Our results are consistent with those of Otálora et al. (2010) showing that a narrow ecological niche may be a driving factor for high specificity, in that *P. malacea* 5 and its reciprocal partner were found only at the northern reaches in our study.

In assessing genetically based specificity with the resulting *Peltigera* haplotype network (Fig. 2) and *Nostoc* phylogenetic tree (Fig. 3 and Appendix S1), our findings are similar to those of Magain et al. (2017a) and O'Brien et al. (2013). Although phylogenetic relationships help predict associations in some cases, this is not a

consistent rule. For example, *Nostoc* phylogroup VIIa associates with relatively closely related species, all from section *Polydactylon* (Figs. 1 and 2). However, *Nostoc* phylogroup IV is found with two *Peltidea* species, *P. malacea* 2 and *P aphthosa*, but also with *P. neopolydactyla* 4, which is a member of section *Polydactylon* (Figs. 1 and 2; Miadlikowska et al., 2014). These relationships may then be mediated by spatial distribution, given that phylogenetically unrelated species that are side-by-side in the transect, such as *P. neopolydactyla* 4 and *P. aphthosa*, can share the same *Nostoc* phylogroup (Fig. 2).

Overall implications

Factors driving patterns of symbiotic associations are scale dependent. Whereas previous studies examined *Peltigera* and other lichen associations at a macroscale (Singh et al., 2016; Magain et al., 2017a) or mostly at a microscale (O'Brien et al., 2013), the present study aimed to assess intermediate, intrabiome patterns. We found *Peltigera* species to be specific, associating with mostly one and sometimes two cyanobiont phylogroups. Although Magain et al. (2017a) showed that at the interbiome scale, environmental factors drive *Nostoc* phylogroup distributions, which then delimit global *Peltigera* species ranges, *Nostoc* availability was not the only driver of *Peltigera* species geographic ranges and association at the intrabiome scale. At this smaller spatial scale, we found that environmental factors seem to be important co-drivers of *Peltigera* species distributions and that the most commonly found *Nostoc* phylogroups have broader ranges than their associating *Peltigera* species. Many *Peltigera* species distributions were restricted to subsections of our transects even when the preferred *Nostoc* phylogroup was more widespread, indicating that regional-scale abiotic factors limit the fungal partner's distribution. Contrary to the mycobiont, in general *Nostoc* ranges were not associated with climatic variables at this intrabiome scale. Within the boreal biome, an increase in the number of *Nostoc* partners was not found to expand the distribution range of the mycobiont.

ACKNOWLEDGEMENTS

The authors thank the Air Saguenay pilot J. Bérubé and the team at Lac Margane for making the sampling across the boreal biome in Québec possible; members of the Lutzoni (Duke University) and A. E. Arnold (University of Arizona) labs for field assistance in Québec, part of the sampling for the Dimensions of Biodiversity project; and two anonymous reviewers for comments and suggestions that improved the manuscript. The sampling, processing, and sequencing of lichen specimens for this project was financially supported by National Science Foundation grants (DEB-1046065 to F.L.; DEB-1025930 and DEB-1556995 to J.M. and F.L.). This work was supported in part by the Swiss National Science Foundation prospective researcher grant PBGEP3_145339 to C.T.

DATA ACCESSIBILITY

The *rbcLX* dataset (410 OTUs) and the resulting most likely tree are available in TreeBASE (http://purl.org/phylo/ treebase/phylows/study/S22406). GenBank accession numbers for sequences generated in this study are included in Appendix 1.

SUPPORTING INFORMATION

Additional Supporting Information may be found online in the supporting information tab for this article.

LITERATURE CITED

Baloch, E., H. T. Lumbsch, and M. Wedin. 2010. Major clades and phylogenetic relationships between lichenized and non-lichenized lineages in Ostraples (Ascomycota: Lecanoromycetes). *Taxon* 59: 1483–1494.

Beck, A., T. Kasalicky, and G. Rambold. 2002. Myco-photobiontal selection in a Mediterranean cryptogam community with *Fulgensia fulgida*. *New Phytologist* 153: 317–326.

Blaha, J., E. Baloch, and M. Grube. 2006. High photobiont diversity associated with the euryoecious lichen-forming ascomycete *Lecanora rupicola* (Lecanoraceae, Ascomycota). *Biological Journal of the Linnean Society* 88: 283–293.

Boucher, D. H., S. James, and K. H. Keeler. 1982. The ecology of mutualism. *Annual Review of Ecology and Systematics* 13: 315–347.

Carpenter, B., A. Gelman, M. D. Hoffman, D. Lee, B. Goodrich, M. Betancourt, M. Brubaker, et al. 2017. Stan: A probabilistic programming language. *Journal of Statistical Software* 76: 1–32.

Chagnon, P.-L., N. Magain, J. Miadlikowska, and F. Lutzoni. 2018. Strong specificity and network modularity at a very fine phylogenetic scale in the lichen genus *Peltigera*. *Oecologia* 187: 767–782.

Clement, M., D. Posada, and K. A. Crandall. 2000. TCS: A computer program to estimate gene genealogies. *Molecular Ecology* 9: 1657–1660.

Cornelissen, J. H. C., T. V. Callaghan, J. M. Alatalo, A. Michelsen, E. Graglia, A. E. Hartley, D. S. Hik, et al. 2001. Global change and arctic ecosystems: Is lichen decline a function of increases in vascular plant biomass? *Journal of Ecology* 89: 984–994.

Darnajoux, R., X. Zhang, D. L. McRose, J. Miadlikowska, F. Lutzoni, A. M. L. Kraepiel, and J.-P. Bellenger. 2017. Biological nitrogen fixation by alternative nitrogenases in boreal cyanolichens: Importance of molybdenum availability and implications for current biological nitrogen fixation estimates. *New Phytologist* 213: 680–689.

de Vienne, D. M., G. Refregier, M. Lopez-Villavicencio, A. Tellier, M. E. Hood, and T. Giraud. 2013. Cospeciation vs host-shift speciation: Methods for testing, evidence from natural associations and relation to coevolution. *New Phytologist* 198: 347–385.

Gardes, M., and T. D. Bruns. 1993. ITS primers with enhanced specificity for basidiomycetes—application to the identification of mycorrhizae and rusts. *Molecular Ecology* 2: 113–118.

Hodkinson, B. P., J. L. Allen, L. Forrest, B. Goffinet, E. Sérusiaux, Ó. S. Andrésson, V. Miao, et al. 2014. Lichen-symbiotic cyanobacteria associated with *Peltigera* have an alternative vanadium-dependent nitrogen fixation system. *European Journal of Phycology* 49: 11–19.

Hodkinson, B. P., N. R. Gottel, C. W. Schadt, and F. Lutzoni. 2012. Photoautotrophic symbiont and geography are major factors affecting highly-structured and diverse bacterial communities in the lichen microbiome. *Environmental Microbiology* 14: 147–161.

Hodkinson, B. P., and F. Lutzoni. 2009. A microbiotic survey of lichen-associated bacteria reveals a new lineage from the Rhizobiales. *Symbiosis* 49: 163–180.

Li, L. A., and L. R. Tabita. 1997. Maximum activity of recombinant ribulose 1,5 bisphosphate carboxylase/oxygenase of *Anabaena* sp. strain CA requires the product of the rbcX gene. *Journal of Bacteriology* 179: 3793–3796.

Lutzoni, F., M. Pagel, and V. Reeb. 2001. Major fungal lineages are derived from lichen symbiotic ancestors. *Nature* 411: 937–940.

Lutzoni, F., P. Wagner, V. Reeb, and S. Zoller. 2000. Integrating ambiguously aligned regions of DNA sequences in phylogenetic analyses without violating positional homology. *Systematic Biology* 49: 628–651.

Maddison, D., and W. Maddison. 2005. MacClade v. 4.08. Sinauer Associates, Sunderland, Massachusetts, USA.

Magain, N., J. Miadlikowska, B. Goffinet, E. Sérusiaux, and F. Lutzoni. 2017a. Macroevolution of specificity in cyanolichens of the genus *Peltigera* section *Polydactylon* (Lecanoromycetes, Ascomycota). *Systematic Biology* 66: 74–99.

Magain, N., J. Miadlikowska, O. Mueller, M. Gajdeczka, C. Truong, A. Salamov, I. Dubchak, et al. 2017b. Conserved genomic collinearity as a source of broadly applicable, fast evolving, markers to resolve species complexes: A case study using the lichen-forming genus *Peltigera* section *Polydactylon*. *Molecular Phylogenetics and Evolution* 117: 10–29.

Miadlikowska, J., and F. Lutzoni. 2000. Phylogenetic revision of the genus *Peltigera* (lichen-forming ascomycetes) based on morphological, chemical and large subunit nuclear ribosomal DNA data. *International Journal of Plant Sciences* 161: 925–958.

Miadlikowska, J., and F. Lutzoni. 2004. Phylogenetic classification of peltigeralean fungi (Peltigerales, Ascomycota) based on ribosomal RNA small and large subunits. *American Journal of Botany* 91: 449–464.

Miadlikowska, J., F. Lutzoni, T. Goward, S. Zoller, and D. Posada. 2003. New approach to an old problem: Incorporating signal from gap-rich regions of ITS and nrDNA large subunit into phylogenetic analyses to resolve the *Peltigera canina* species complex. *Mycologia* 95: 1181–1203.

Miadlikowska, J., D. Richardson, N. Magain, B. Ball, F. Anderson, R. Cameron, J. Lendemer, et al. 2014. Phylogenetic placement, species delimitation, and cyanobiont identity of endangered aquatic *Peltigera* species (lichen-forming Ascomycota, Lecanoromycetes). *American Journal of Botany* 101: 1141–1156.

Miller, M. A., W. Pfeiffer, and T. Schwartz. 2010. Creating the CIPRES Science Gateway for inference of large phylogenetic trees. Gateway Computing Environments Workshop (GCE), 2010, IEEE.

Myllys, L., S. Stenroos, A. Thell, and M. Kuusinen. 2006. High cyanobiont selectivity of epiphytic lichens in old growth boreal forest in Finland. *New Phytologist* 173: 621–629.

Nash, T. H. 2008. Lichen biology. Cambridge University Press, Cambridge, UK.

Nelsen, M. P., and A. Gargas. 2009. Symbiont flexibility in (Pertusariales: Icmadophilaceae). *The Bryologist* 112: 404–417.

O'Brien, H. E., J. Miadlikowska, and F. Lutzoni. 2005. Assessing host specialization in symbiotic cyanobacteria associated with four closely related species of the lichen fungus *Peltigera*. *European Journal of Phycology* 40: 363–378.

O'Brien, H. E., J. Miadlikowska, and F. Lutzoni. 2009. Assessing reproductive isolation in highly diverse communities of the lichen-forming fungus genus *Peltigera*. *Evolution* 63: 2076–2086.

O'Brien, H. E., J. Miadlikowska, and F. Lutzoni. 2013. Assessing population structure and host specialization in lichenized cyanobacteria. *New Phytologist* 198: 557–566.

Otálora, M. A., G. Aragón, I. Martínez, and M. Wedin. 2013. Cardinal characters on a slippery slope: A re-evaluation of phylogeny, character evolution, and evolutionary rates in the jelly lichens (Collemataceae s. str). *Molecular Phylogenetics and Evolution* 68: 185–198.

Otálora, M. A., I. Martínez, H. O'Brien, M. C. Molina, G. Aragon, and F. Lutzoni. 2010. Multiple origins of high reciprocal symbiotic specificity at an intercontinental spatial scale among gelatinous lichens (Collemataceae, Lecanoromycetes). *Molecular Phylogenetics and Evolution* 56: 1089–1095.

Paulsrud, P., and P. Lindblad. 1998. Sequence variation of the tRNA Leu Intron as a marker for genetic diversity and specifcity of symbiotic cyanobacteria in some lichens. *Applied and Environmental Microbiology* 64: 310–315.

Peksa, O., and P. Škaloud. 2011. Do photobionts influence the ecology of lichens? A case study of environmental preferences in symbiotic green alga *Asterochloris* (Trebouxiophyceae). *Molecular Ecology* 20: 3936–3948.

Pérez-Ortega, S., R. Ortiz-Álvarez, T. G. A. Green, and A. de Los Ríos. 2012. Lichen myco-and photobiont diversity and their relationships at the edge of life (McMurdo Dry Valleys, Antarctica). *FEMS Microbiology Ecology* 82: 429–448.

Rodríguez, F. J., J. L. Oliver, A. Marín, and J. R. Medina. 1990. The general stochastic model of nucleotide substitution. *Journal of Theoretical Biology* 142: 485–501.

Rudi, K., O. M. Skulberg, and K. S. Jakobsen. 1998. Evolution of cyanobacteria by exchange of genetic material among phyletically related strains. *Journal of Bacteriology* 180: 3453–3461.

Schoch, C. L., K. A. Seifert, S. Huhndorf, V. Robert, J. L. Spouge, C. A. Levesque, and W. Chen. 2012. Nuclear ribosomal internal transcribed spacer (ITS) region as a universal DNA barcode marker for Fungi. *Proceedings of the National Academy of Sciences USA* 109: 6241–6246.

Singh, G., F. Dal Grande, P. K. Divakar, J. Otte, A. Crespo, and I. Schmitt. 2016. Fungal-algal association patterns in lichen symbiosis linked to macroclimate. *New Phytologist* 214: 317–329.

Spribille, T., V. Tuovinen, P. Resl, D. Vanderpool, H. Wolinski, M. C. Aime, K. Schneider, et al. 2016. Basidiomycete yeasts in the cortex of ascomycete macrolichens. *Science* 353: 488–492.

Stamatakis, A. 2006. RAxML-VI-HPC: Maximum likelihood-based phylogenetic analyses with thousands of taxa and mixed models. *Bioinformatics* 22: 2688–2690.

Stamatakis, A., P. Hoover, and J. Rougemont. 2008. A rapid bootstrap algorithm for the RAxML Web servers. *Systematic Biology* 57: 758–771.

Stan Development Team. 2017. RStan: The R interface to Stan. R package version 2.16.2. http://mc-stan.org.

Thompson, J. N. 2005. The geographic mosaic of evolution. University of Chicago Press, Chicago, Illinois, USA.

Vasquez, D. P., C. J. Melián, N. M. Williams, N. Blüthen, B. R. Krasnov, and R. Poulin. 2007. Species abundance and asymmetrical interaction strength in ecological networks. *Oikos* 116: 1120–1127.

Vermeji, G. J. 1999. Inequality and the directionality of history. *The American Naturalist* 153: 243–253.

Vermeji, G. J. 2004. Nature: An economic history. Princeton University Press, Princeton, New Jersey, USA.

Wedin, M., H. Döring, and G. Gilenstam. 2004. Saprotrophy and lichenization as options for the same fungal species on different substrata: Environmental plasticity and fungal lifestyles in the *Stictis-Conotrema* complex. *New Phytologist* 164: 459–465.

Werth, S., and D. Fontaneto. 2011. Biogeography and phylogeography of lichen fungi and their photobionts. *In* D. Fontaneto [ed.], Biogeography of micro-organisms: Is everything small everywhere? 191–208. Cambridge University Press, Cambridge, UK.

Wheeler, D. L., T. Barrett, D. A. Benson, S. H. Bryant, K. Canese, V. Chetvernin, D. M. Church, et al. 2007. Database resources of the national center for biotechnology information. *Nucleic Acids Research* 35: D5–D12.

White, T. J., T. Bruns, S. Lee, and J. Taylor. 1990. Amplification and direct sequencing of fungal ribosomal RNA genes for phylogenetics. *PCR Protocols: A Guide to Methods and Applications* 18: 315–322.

Wilson, D. S., and J. Yoshimura. 1994. On the coexistence of specialists and generalists. *American Naturalist* 144: 692–707.

Wirtz, N., H. T. Lumbsch, T. G. Green, R. Türk, A. Pintado, L. Sancho, and B. Schroeter. 2003. Lichen fungi have low cyanobiont selectivity in maritime Antarctica. *New Phytologist* 160: 177–183.

Yahr, R., R. Vilgalys, and P. T. Depriest. 2004. Strong fungal specificity and selectivity for algal symbionts in Florida scrub *Cladonia* lichens. *Molecular Ecology* 13: 3367–3378.

Zolan, M., and P. Pukkila. 1986. Inheritance of DNA methylation in *Coprinus cinereus*. *Molecular and Cellular Biology* 6: 195–200.

Zúñiga, C., D. Leiva, M. Carú, and J. Orlando. 2017. Substrates of *Peltigera* lichens as a potential source of cyanobionts. *Microbial Ecology* 74: 561–569.

APPENDIX 1. Taxon sampling of *Peltigera* on the south–north (SN) and east–west (EW) transects (Fig. 1) in Québec, Canada.

Specimen ID	Taxon	Locality, site, and cluster	Coordinates	ITS	*rbcLX*	*Peltigera* haplotype	*Nostoc* phylogroup
P5057	*Peltigera aphthosa*	SN5_C2	52.41264°N, 73.07248°W	MG811733	MG818406	1	IV
P5053	*P. aphthosa*	SN8_E1	56.53598°N, 73.22478°W	MG811732	MG818411	1	IV
P5002	*P. aphthosa*	SN8_E2	56.53636°N, 73.22427°W	MG811728	MG818409	1	IV
P5007	*P. aphthosa*	SN8_E3	56.53677°N, 73.22429°W	MG811731	MG818412	3	IV
P5046	*P. aphthosa*	SN9_C1	57.91270°N, 72.97673°W	MG811737	MG818434	4	IV
P5054	*P. aphthosa*	SN9_W1	57.96773°N, 73.04319°W	MG811738	MG818436	4	IV
P5005	*P. aphthosa*	W12.5_C2	50.95784°N, 68.71450°W	MG811730	MG818408	2	IV
P5003	*P. aphthosa*	W12.5_C3	50.95783°N, 68.71523°W	MG811729	MG818407	1	IV
P5084	*P. aphthosa*	E100_C1	51.13508°N, 66.04708°W	MG811734	MG818433	1	IV
P5086	*P. aphthosa*	E200_C2	51.28011°N, 63.83678°W	MG811735	Missing	1	n/a
P5080	*P. aphthosa*	W100_C1	50.79232°N, 70.74293°W	MG811736	MG818439	1	IV
P0741	*P. aphthosa*	W1.5_C1	51.08493°N, 68.53860°W	MG811726	MG818432	1	IV
P0727	*P. aphthosa*	W6_C1	51.03429°N, 68.60778°W	MG811727	MG818438	1	IV
P5056	*P. aphthosa*	SN4_E2	51.06926°N, 73.03429°W	Missing	MG818410	n/a	IV
P0735	*P. malacea* 2	SN6_E2	53.86195°N, 72.99868°W	MG811718	MG818374	1	IV
P5044	*P. malacea* 2	SN6_E3	53.86195°N, 72.99868°W	MG811720	MG818375	2	IV
P5063	*P. malacea* 2	W3_C3	51.06652°N, 68.55525°W	MG811721	MG818376	2	IV
P5004	*P. malacea* 2	SN8_C1	56.52742°N, 73.27129°W	MG811719	MG818377	1	IV
P5006	*P. malacea* 5	SN8_W2	56.53179°N, 73.34526°W	MG811723	MG818379	3	III
P0737	*P. malacea* 5	SN8_W3	56.53210°N, 73.34454°W	MG811725	MG818378	3	III
P5047	*P. malacea* 5	SN9_C1	57.91270°N, 72.97673°W	MG811724	MG818381	3	III
P5000	*P. malacea* 5	SN9_W1	57.96773°N, 73.04319°W	MG811722	MG818380	3	III
P5025	*P. neopolydactyla* 1	SN3_W2	49.34304°N, 73.40994°W	MG811754	MG818425	1	VIIa
P5016	*P. neopolydactyla* 1	SN3_E1	49.39553°N, 73.46278°W	MG811751	MG818382	1	VIIa
P5015	*P. neopolydactyla* 1	SN3_C1	49.36126°N, 73.44313°W	MG811750	MG818431	1	VIIa
P0303	*P. neopolydactyla* 1	SN3_C1	49.36126°N, 73.44313°W	MG811740	MG818385	1	VIIa
P5024	*P. neopolydactyla* 1	SN3_E1	49.39553°N, 73.46278°W	MG811752	MG818383	1	VIIa
P5042	*P. neopolydactyla* 1	SN5_W1	52.39765°N, 73.09985°W	MG811755	MG818426	1	VIIa
P0317	*P. neopolydactyla* 1	SN6_E3	53.86195°N, 72.99868°W	MG811744	MG818386	1	VIIa
P0324	*P. neopolydactyla* 1	W1.5_C1	51.08493°N, 68.53860°W	MG811748	MG818384	1	VIIa
P0319	*P. neopolydactyla* 1	W100_C2	50.79128°N, 70.74345°W	MG811745	MG818391	1	VIIa
P0323	*P. neopolydactyla* 1	W25_C1	50.92852°N, 68.97288°W	MG811747	MG818387	1	VIIa
P0313	*P. neopolydactyla* 1	W25_C2	50.92820°N, 68.97259°W	MG811743	MG818389	1	VIIa
P5061	*P. neopolydactyla* 1	E100_C3	51.13462°N, 66.04774°W	MG811749	MG818430	1	VIIa
P5083	*P. neopolydactyla* 1	E100_C1	51.13508°N, 66.04708°W	MG811753	MG818429	1	VIIa
P0300	*P. neopolydactyla* 1	W3_C1	51.06635°N, 68.55641°W	MG811739	MG818388	1	VIIa
P0309	*P. neopolydactyla* 1	W50_C1	50.89513°N, 69.50816°W	KX897220	KX922922	1	VIIa
P0307	*P. neopolydactyla* 1	W50_C2	50.89483°N, 69.50854°W	MG811742	MG818428	1	VIIa
P0322	*P. neopolydactyla* 1	W6_C2	51.03423°N, 68.60746°W	MG811746	MG818427	1	VIIa
P0304	*P. neopolydactyla* 1	W100_C1	50.79232°N, 70.74293°W	MG811741	MG818390	1	VIIa
P0320	*P. neopolydactyla* 4	E100_C2	51.13479°N, 66.04754°W	MG811757	MG818404	1	IV
P5082	*P. neopolydactyla* 4	W100_C1	50.79232°N, 70.74293°W	MG811759	MG818416	2	XIa
P0321	*P. neopolydactyla* 4	E200_C1	51.28066°N, 63.83717°W	KX897253	KX922949	1	IV
P5026	*P. neopolydactyla* 4	E200_C3	51.27972°N, 63.83693°W	MG811756	MG818405	1	IV
P5014	*P. neopolydactyla* 4	SN2_E1	47.91781°N, W72.96183	MG811758	MG818403	1	IV
P0302	*P. neopolydactyla* 4	SN2_W1	47.89268°N, 72.89707°W	KX897252	KX922948	1	IV
P5062	*P. occidentalis*	E200_C1	51.28066°N, 63.83717°W	MG811762	MG818435	1	VIIa
P0299	*P. occidentalis*	SN5_C1	52.41323°N, 73.07322°W	KX897269	KX922965	1	VIIa
P0305	*P. occidentalis*	SN5_C3	52.41315°N, 73.07139°W	MG811763	MG818422	1	VIIa
P0314	*P. occidentalis*	SN8_C3	56.52835°N, 73.27141°W	KX897270	KX922966	1	VIIa
P5048	*P. occidentalis*	SN9_C1	57.91270°N, 72.97673°W	MG811760	MG818447	1	VIIa
P0316	*P. occidentalis*	SN9_E1	57.88662°N, 73.02011°W	MG811764	MG818448	1	VIIa
P0108	*P. occidentalis*	W1.5_C3	51.08519°N, 68.53794°W	KX897268	KX922964	1	VIIa
P5081	*P. occidentalis*	W100_C1	50.79232°N, 70.74293°W	MG811765	MG818420	1	VIIa
P0103	*P. occidentalis*	SN5_W3	52.39718°N, 73.10094°W	MG811761	MG818421	1	VIIa
P5033	*P. scabrosa* 1	EW0_C1	51.10506°N, 68.52175°W	MG811779	MG818445	1	VIIa
P5027	*P. scabrosa* 1	SN3_W1	49.34324°N, 73.41033°W	MG811783	MG818398	1	VIIa
P5022	*P. scabrosa* 1	SN3_W3	49.34311°N, 73.41059°W	MG811780	MG818397	1	VIIa
P5020	*P. scabrosa* 1	SN5_C2	52.41264°N, 73.07248°W	MG811782	MG818395	1	VIIa
P5021	*P. scabrosa* 1	SN5_E3	52.42619°N, 73.03578°W	MG811781	MG818401	1	VIIa
P5017	*P. scabrosa* 1	SN6_W1	53.79902°N, 73.07108°W	MG811777	MG818402	1	VIIa

(continued)

APPENDIX 1. (Continued)

Specimen ID	Taxon	Locality, site, and cluster	Coordinates	ITS	*rbcLX*	*Peltigera* haplotype	*Nostoc* phylogroup
P5009	*P. scabrosa* 1	SN7_C1	55.16037°N, 73.33066°W	MG811776	MG818400	1	VIIa
P5010	*P. scabrosa* 1	SN7_W1	55.16028°N, 73.28°W	MG811775	MG818394	1	VIIa
P5019	*P. scabrosa* 1	SN8_C3	56.52835°N, 73.27141°W	MG811778	MG818396	1	VIIa
P5085	*P. scabrosa* 1	E100_C2	51.13479°N, 66.04754°W	MG811772	missing	2	n/a
P5032	*P. scabrosa* 1	E50_C1	51.08765°N, 67.22046°W	MG811773	MG818444	2	VIIa
P5034	*P. scabrosa* 1	EW0_C2	51.10470°N, 68.52167°W	MG811774	MG818443	2	VIIa
P0097	*P. scabrosa* 1	SN2_E1	47.91781°N, 72.96183°W	KX897307	KX923000	1	VIIa
P0095	*P. scabrosa* 1	SN2_E2	47.91811°N, 72.96188°W	MG811767	MG818440	1	VIIa
P0310	*P. scabrosa* 1	SN5_C3	52.41315°N, 73.07139°W	MG811768	MG818393	1	VIIa
P0311	*P. scabrosa* 1	SN6_W3	53.79826°N, 73.07170°W	KX897305	KX922998	1	VIIa
P0306	*P. scabrosa* 1	SN6_W3	53.79826°N, 73.07170°W	KX897304	KX922997	1	VIIa
P0308	*P. scabrosa* 1	SN7_C1	55.16037°N, 73.33066°W	MG811769	MG818392	1	VIIa
P0094	*P. scabrosa* 1	W1.5_C1	51.08493°N, 68.53860°W	MG811766	MG818442	1	VIIa
P0093	*P. scabrosa* 1	W25_C1	50.92852°N, 68.97288°W	KX897306	KX922999	1	VIIa
P0297	*P. scabrosa* 1	W1.5_C2	51.08504°N, 68.53794°W	MG811771	MG818424	2	VIIa
P0301	*P. scabrosa* 1	W100_C1	50.79232°N, 70.74293°W	MG811770	MG818399	1	VIIa
P0091	*P. scabrosa* 1	E100_C1	51.13508°N, 66.04708°W	Missing	MG818441	n/a	VIIa
P0107	*P. scabrosa* 2	SN8_E2	56.53636°N, 73.22427°W	KX897310	KX923003	3	XIa
P5060	*P.* cf. *scabrosa* 2	E200_C1	51.28066°N, 63.83717°W	Missing	MG818417	n/a	XIa
P5018	*P. scabrosa* 2	SN8_E2	56.53636°N, 73.22427°W	MG811784	MG818414	1	XIa
P0296	*P. scabrosa* 2	SN8_E3	56.53677°N, 73.22429°W	KX897315	KX923008	1	XIa
P0113	*P. scabrosa* 2	SN8_W1	56.53144°N, 73.34532°W	KX897311	KX923004	1	XIa
P5045	*P. scabrosa* 2	SN9_C1	57.91270°N, 72.97673°W	MG811788	MG818437	3	VIId
P5023	*P. scabrosa* 2	SN9_C2	57.91304°N, 72.07611°W	MG811786	MG818413	3	VIId
P5012	*P. scabrosa* 2	SN9_C3	57.91331°N, 72.97562°W	MG811785	MG818415	3	XIa
P5013	*P. scabrosa* 2	SN9_E2	57.88679°N, 73.01962°W	MG811787	MG818418	1	XIa
P5031	*P. scabrosa* 2	SN9_W3	57.96691°N, 73.04353°W	MG811789	MG818419	2	XIa
P0312	*P. scabrosa* 4	SN6_E1	53.86235°N, 72.99900°W	KX897323	KX923016	1	VIIa
P0318	*P. scabrosa* 4	SN6_W2	53.79826°N, 73.07170°W	KX897325	KX923018	1	VIIa
P5011	*P. scabrosa* 4	SN8_C1	56.52742°N, 73.27129°W	MG811790	MG818423	1	VIIa
P0315	*P. scabrosa* 4	SN9_C1	57.91270°N, 72.97673°W	KX897324	KX923017	1	VIIa
P5029	*P. scabrosa* 4	SN9_C1	57.91270°N, 72.97673°W	MG811791	MG818446	1	VIIa

Notes: Most voucher specimens were collected by J. Miadlikowska and F. Lutzoni and are deposited at Duke University herbarium (DUKE). GenBank accession numbers beginning with MG represent newly acquired ITS and *rbcLX* sequences. Haplotype numbers refer to specific haplotypes in haplotype networks within a *Peltigera* species, or closely related species, based on ITS (Fig. 2). Phylogroup roman numerals refer to *Nostoc* monophyletic groups based on *rbcLX* sequences (Fig. 3), which can serve as a proxy for species, and are consistent with Magain et al. (2017a). *Peltigera* species are numbered following species delimitations by Magain et al. (2017b) and J. Miadlikowska (unpublished data). n/a = not applicable.